Heliyon 10 (2024) e38447

Contents lists available at ScienceDirect

Heliyon

journal homepage: www.cell.com/heliyon

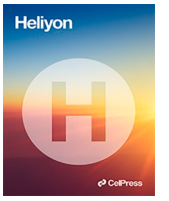

Research article

Generation of *ex vivo* autologous hematopoietic stem cell-derived T lymphocytes for cancer immunotherapy

Kajornkiat Maneechai [a,b,d], Wannakorn Khopanlert [a,b,c,d], Panarat Noiperm [a,d], Phakaporn Udomsak [a,d], Pongtep Viboonjuntra [a], Jakrawadee Julamanee [a,d,*]

[a] *Stem Cell Laboratory, Hematology Unit, Division of Internal Medicine, Faculty of Medicine, Prince of Songkla University, Hat Yai, Songkhla 90110, Thailand*
[b] *Department of Biomedical Sciences and Biomedical Engineering, Faculty of Medicine, Prince of Songkla University, Hat Yai, Songkhla 90110, Thailand*
[c] *Anatomical Pathology Unit, Division of Pathology, Faculty of Medicine, Prince of Songkla University, Hat Yai, Songkhla 90110, Thailand*
[d] *Thailand Hub of Talents in Cancer Immunotherapy (TTCI), Thailand*

ARTICLE INFO

Keywords:
Autologous
Hematopoietic stem cells
T lymphocyte
Adoptive T-cell therapy

ABSTRACT

CD19CAR-T cell therapy demonstrated promising outcomes in relapsed/refractory B-cell malignancies. Nonetheless, the limited T-cell function and ineffective T-cell apheresis for therapeutic purposes are still concern in heavily pretreated patients. We investigated the feasibility of generating hematopoietic stem cell-derived T lymphocytes (HSC-T) for cancer immunotherapy. The patients' autologous peripheral blood HSCs were enriched for $CD34^+$ and $CD3^+$ cells. The $CD34^+$ cells were then cultured following three steps of lymphoid progenitor differentiation, T-cell differentiation, and T-cell maturation processes. HSC-T cells were successfully generated with robust fold expansion of 3735 times. After lymphoid progenitor differentiation, $CD5^+$ and $CD7^+$ cells remarkably increased (65–84 %) while $CD34^+$ cells consequentially declined. The mature $CD3^+$ cells were detected up to 40 % and 90 % on days 42 and 52, respectively. The majority of HSC-T population was naïve phenotype compared to CD3-T cells (73 % vs 34 %) and CD8:CD4 ratio was 2:1. The higher level of cytokine and cytotoxic granule secretion in HSC-T was observed after activation. HSC-T cells were assessed for clinical application and found that CD19CAR-transduced HSC-T cells demonstrated higher cytokine secretion and a trend of superior cytotoxicity against $CD19^+$ target cells compared to control CAR-T cells. A chronic antigen stimulation assay revealed similar T-cell proliferation, stemness, and exhaustion phenotypes among CAR-T cell types. In conclusions, autologous HSC-T was feasible to generate with preserved T-cell efficacy. The HSC-T cells are potentially utilized as an alternative option for cellular immunotherapy.

1. Background

Adoptive T-cell therapy (ACT) has emerged as an effective personalized treatment strategy, especially chimeric antigen receptor (CAR)-T cell therapy. T lymphocytes engineered to express anti-CD19CAR demonstrated promising clinical outcomes across various

* Corresponding author. Stem Cell Laboratory, Hematology Unit, Division of Internal Medicine, Faculty of Medicine, Prince of Songkla University, Hat Yai, Songkhla 90110, Thailand.
E-mail addresses: jjakrawadee@gmail.com, jakrawadee.j@psu.ac.th (J. Julamanee).

https://doi.org/10.1016/j.heliyon.2024.e38447
Received 4 May 2024; Received in revised form 20 September 2024; Accepted 24 September 2024
Available online 25 September 2024

clinical trials and real-world studies, which led to an approval by the United States Food and Drug Administration and altered treatment paradigms for relapsed/refractory B-cell malignancies [1–12]. Despite the promising results, there are still challenges including ineffective T-cell functions from heavy chemotherapy and/or radiotherapy of pre-exposed individuals as well as inadequate apheresis T-cell products for therapeutic purposes [9,13,14].

To alleviate these obstacles, various strategies have been proposed to provide an alternative immune cell source for ACT. Allogeneic donor-derived T-cell products have been employed under genetic modification to overcome human leukocyte antigen (HLA)-mismatch between donor and recipient [15]. Genome editing to disrupt the T-cell receptor (TCR) gene is commonly performed to prevent the risk of graft-versus-host disease (GvHD) and turn these modified cells into a "universal T-cell product". However, this strategy is mainly limited in clinical settings and long-term unforeseen consequences related to gene modification are of crucial concern [15,16]. Allogeneic natural killer (NK) or γδ T-cells are also feasible innate immune cell sources, and their clinical efficacies and safety profiles were previously reported [17–20]. Additionally, induced pluripotent stem cells (iPSCs), which plausibly provide an endless supply of T-cells, have gained popularity. T- and NK-derived human iPSCs have been studied in early phase clinical trials that demonstrated their safety and continued clinical benefit in B-cell lymphoma [21–28].

Another plausible strategy would be generating *ex vivo* T lymphocytes from hematopoietic stem cells (HSCs). HSCs are a special type of human cell that can divide and differentiate into various hematopoietic cell lineages and are known for their ability to self-renew. Umbilical cord blood (UCB) and bone marrow (BM) are sources of plentiful HSCs to produce T lymphocytes. UCB-derived HSCs contain a higher proliferative capacity with less mature T-cell contamination, which can result in a greater yield for cellular immunotherapy. Manufacturing a $CD8^+$ T lymphocyte product from UCB-derived HSCs requires many steps and several cytokines and, in the end, it would not be suitable as a universal ACT [29–31]. Apheresis of peripheral blood HSCs (PBSCs) following colony-stimulating factor stimulation is a more simplified option and provides a sufficient quantity of HSCs [30,32–34].

T-cells are primarily differentiated in the thymus, where thymic epithelial cells (TECs) expressing Delta-like 4 (DLL4) interact with the Notch-1 receptor in a certain milieu [35,36]. To mimic *in vivo* development, co-culturing of OP9 murine stromal cells transduced to express Notch ligand, Delta-like-4 (OP9-DL4) or Delta-like-1 (OP9-DL1), with HSCs in the presence of FMS-like tyrosine kinase 3 ligand (Flt3L), stem cell factor (SCF), and interleukin (IL)-7 was developed to allow *in vitro* generation of human T-cells [37–39]. Since the stromal co-culture system is rely on the use of murine stromal cells and serum-containing medium, it may limit this approach for clinical translation. Recently, the stromal cell-free system has been developed using plate-bound Notch ligands fused to antibody Fc region [29,40,41]. The immobilized Notch ligand-coated plate enabled to promote UCB and HSCs differentiation. However, most of the differentiated cells were $CD8^+$ T-cells which are not suitable for cancer immunotherapy [29].

To overcome the clinical unmet need, the present study aimed to evaluate the potential of generating *ex vivo* autologous T lymphocytes from patient-derived PBSCs using stromal cell-free culture system and provide the functional aspects of HSC-derived T lymphocytes (HSC-T) compared to peripheral blood (PB)-derived T-cells (CD3-T). Additionally, we also generated HSC- and CD3-derived CD19CAR-T cells to assess the clinical application and determine the feasibility of an alternative autologous HSC-derived T lymphocyte product for cancer immunotherapy.

2. Materials and methods

2.1. Cell lines

Raji (Burkitt lymphoma cell line), Nalm-6 (B-cell acute lymphoblastic leukemia cell line), K562 engineered to express CD19 (CD19-K562 cell line), and Ebstein Barr virus (EBV)-transformed lymphoblastoid (EBV-LCL) cell line are maintained and utilized as target or feeder cells for CD19CAR-T cell expansion. Primary mantle cell lymphoma cells were obtained from the peripheral blood of a MCL patient after written informed consent in accordance with the Declaration of Helsinki. Medium containing RPMI-1640 (Gibco, Life Technologies Corp., CA, USA) supplemented with 10 % fetal bovine serum, 1 % L-glutamine, and 1 % penicillin-streptomycin were used to maintain cell lines. Primary cells were cultured in T lymphocyte medium (RPMI-1640 supplemented with 10 % human serum, 2 % L-glutamine, 1 % penicillin-streptomycin, and 0.5 μM 2-mercaptoethanol). All cells were incubated at 37 °C in a humidified atmosphere containing 5 % CO_2.

2.2. Cell isolation

Apheresis HSC products were obtained from a healthy donor or multiple myeloma or lymphoma patients who underwent stem cell transplantation. To isolate $CD3^+$ and $CD34^+$ cells, the PBSCs were incubated with EL buffer (QIAGEN GmBH, Germany) for erythrocyte lysis before isolation. The cells were then isolated using the Lymphoprep™ density gradient centrifugation method (STEMCELL Technologies Inc., Canada) through a mononucleated layer. The $CD34^+$ and $CD3^+$ cells were separately isolated using anti-human CD34 and anti-human CD3 immunomagnetic beads (Miltenyi Biotec, Bergisch Gladbach, Germany), respectively. The enriched cells were assessed for purity using FACS Aria™ Fusion (BD Biosciences, NJ, USA) and were then processed to generate T lymphocytes or cryopreserved until use.

2.3. HSC-derived T lymphocyte generation

The HSC-T generation protocol is composed of three steps of a lymphoid progenitor differentiation phase (days 0–14), T-cell progenitor maturation phase (days 14–42) [29], and single-positive T-cell maturation phase (days 42–52) (Fig. 1A). First, the enriched

HSCs (2.5×10^4 cells) were cultured using StemSpan™ SFEM II medium supplemented with Lymphoid Progenitor Expansion Supplement (STEMCELL™ Technologies, Vancouver, Canada) that contained SCF, thrombopoietin, Flt3L, and IL-7 onto a pre-coated StemSpan™ Lymphoid Differentiation Coating Material non-tissue culture 24-well plate. On day 14, the differentiated progenitor T-cells were collected, counted (5×10^4 cells), and re-plated onto a new pre-coated non-tissue culture 24-well plate containing SFEM II medium supplemented with T Cell Progenitor Maturation Supplement (containing Flt3L and IL-7) for an additional 14 days of culture. On day 28, the differentiated cells were harvested, counted (2.5×10^5), and re-seeded with the same protocol as day 14. On day 42, differentiated cells were harvested, counted, and induced for the final stage of single-positive T-cell differentiation and functional maturity with our optimized protocol by co-culturing 5×10^5 harvested cells with anti-CD3/CD28 beads (Invitrogen, Carlsbad, CA, USA) at a 1:1 ratio and cultured in T lymphocyte medium with IL-2 50 IU/mL supplementation for 10 days. On day 52, the mature T-cells were ready to harvest, count, and use for downstream experiments. At each step of HSC-T generation, an aliquot of cells at the

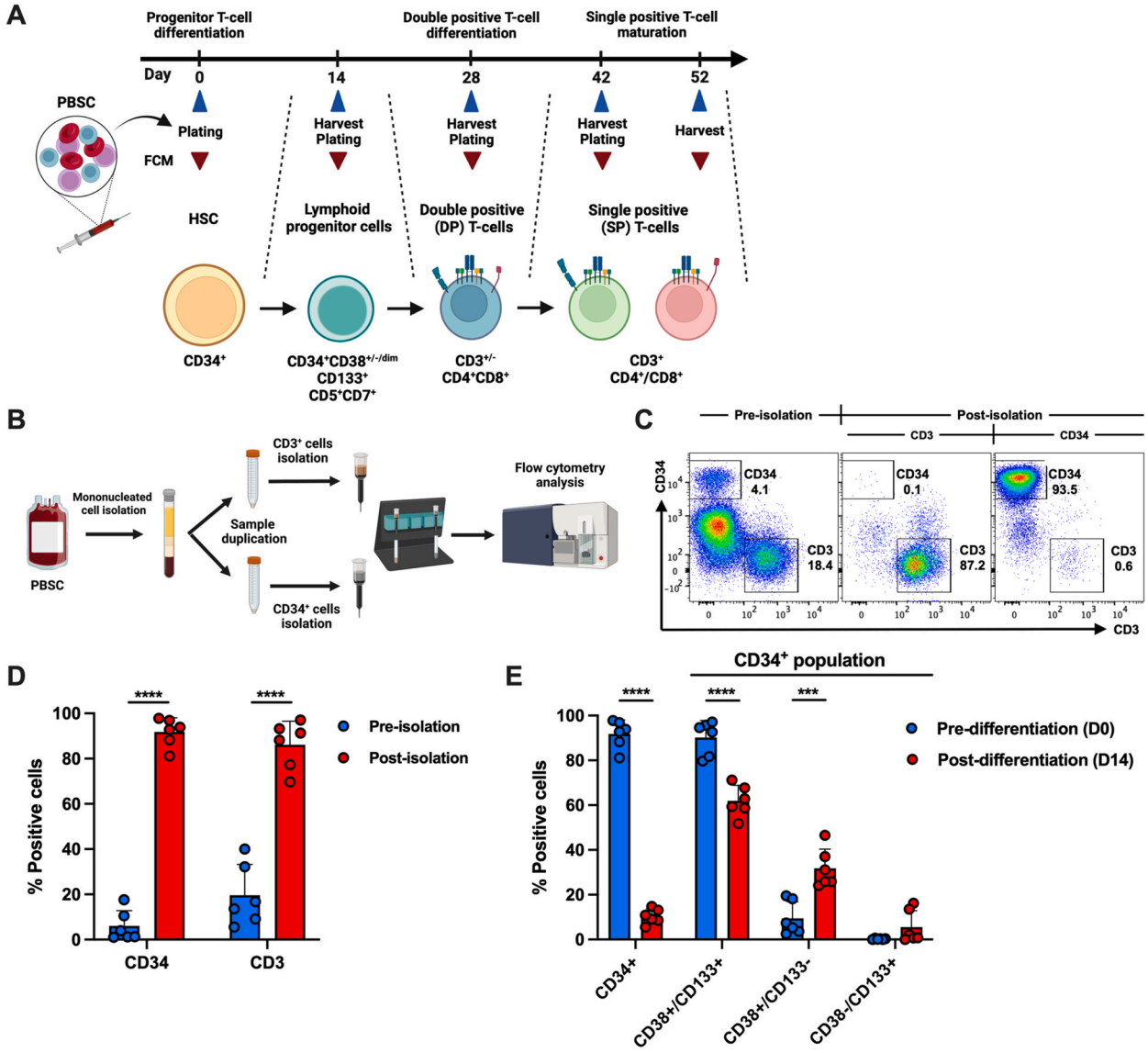

Fig. 1. Hematopoietic stem cell (HSC)-derived T lymphocyte generation. (A) Schematic of HSC-T generation protocol composed of three steps: 1. lymphoid progenitor differentiation phase (days 0–14), 2. T-cell progenitor maturation phase (days 14–42), and 3. single-positive T-cell maturation (days 42–52). PBSC, peripheral blood stem cell; FCM, flow cytometry. (B) Schematic of PBSC isolation (C) Representative flow plots of pre- and post-isolation: PBSC (left), $CD3^+$ cells (middle) and $CD34^+$ cells (right). (D) Percentages of $CD34^+$ and $CD3^+$ cells pre- and post-selection. (E) Percentages of HSC differentiation subsets at pre- (day 0) and post-differentiation (day 14). The HSC differentiation subsets are divided into $CD38^+/CD133^+$ (common lymphoid progenitor [CLP]), $CD38^+/CD133^-$ (erythro-myeloid progenitor [EMP]), and $CD38^-/CD133^+$ (lymphoid-primed multipotent progenitor [LMPP]). Data are pooled from six different samples and presented as mean ± SD. Student's *t*-test for (D) and (E); $^{***}P < 0.001$, $^{****}P < 0.0001$.

indicated time points were assessed for immunophenotypes by flow cytometry.

2.4. CD19CAR T-cell generation

The third-generation CD19CAR incorporated CD28/CD40 co-stimulatory domain (CD19.28.40z CAR) was established by our laboratory [42] and used to test the HSC-T clinical application. Briefly, the CD19CAR single-chain variable fragment (scFv), which is based on the FMC63 clone, was fused to the scFv-IgG4/hinge, CD28 transmembrane, CD28/CD40 co-stimulatory domain, and followed by the CD3ζ intracellular domain. To evaluate transduction efficacy and selection, a self-cleaving T2A ribosomal skip sequence followed by truncated form of the epidermal growth factor receptor (tEGFR) was ligated to CAR structure. Gamma retroviral particles of the CD19.28.40z CAR gene were produced using the retroviral packaging cell line (Phoenix-Ampho, Orbigen, San Diego, CA, USA) as classified elsewhere [43]. HSC-T or CD3-T cells were cultured with anti-CD3/CD28 beads at a 1:1 ratio in T lymphocyte medium supplemented with IL-2. On day 3, activated T-cells were centrifuged at 2100 rpm for 1 h at 32 °C on a retroviral-coated plate (Retronectin, Takara Bio, Otsu, Japan) for transduction. Transduced cells were refreshed with new T lymphocyte medium with the addition of IL-2 and cultured for 7 days. $CD19CAR^+$ T-cells were assessed and isolated using biotin-conjugated anti-EGFR monoclonal antibody (R&D Systems, Minneapolis, MN, USA) followed by counterstaining with anti-biotin microbeads (Miltenyi Biotec, Bergisch Gladbach, Germany). The enriched CAR^+ cells were assessed by flow cytometry and then cultured with γ-irradiated EBV-LCL as feeder cells at an effector (E) to target (T) cell ratio of 1:7 for 8–10 days until a sufficient cell number was achieved for further experiments.

2.5. T-cell immunophenotype assay

HSCs or T-cells were stained with monoclonal antibodies: CD3, CD4, CD5, CD7, CD8, CD34, CD38, CD45RA, CD62L, CD95, CD133, PD-1, LAG-3, granzyme B, perforin, and TCRα/β (BioLegend, San Diego, CA, USA), CCR7, IL-2, IFN- γ, CTLA-4, and TIM-3 (BD Biosciences, NJ, USA). All cell samples were analyzed using FACSAria™ Fusion (BD Biosciences, NJ, USA) and data were analyzed by FlowJo software (Tree Star, OR, USA).

2.6. Intracellular cytokine staining (ICCS) assay

T-cells were activated with anti-CD3/CD28 beads at a 1:1 ratio for 4 h. After 1.5 h of incubation, GolgiPlug™ Protein Transport Inhibitor (BD Biosciences, NJ, USA) was added to the cell suspension. The incubated cells were fixed and permeabilized with Cytofix/Cytoperm™ (BD Biosciences, NJ, USA), then intracellular stained for IFN-γ, IL-2, granzyme-B, and perforin. The stained cells were analyzed by flow cytometry. For CD19CAR-T cell ICCS, untransduced-T or CD19CAR-T cells were co-cultured with CD19-K562 cells at E:T ratio of 1:2 and processed with a similar protocol.

2.7. CAR-T cell proliferation assay

The CAR-T cell proliferative capacity following specific antigen exposure (CD19 antigen) was assessed by co-culturing T-cells with γ-irradiated CD19-K562 at a 1:1 ratio with or without IL-2 supplementation for 14 days. To evaluate T-cell proliferation, the viable cells were counted using trypan blue staining at specific time points.

2.8. CAR-T cytotoxicity assay

Untransduced-T or CD19CAR-T cells were pre-stained with CellTrace Violet (CTV) dye (Invitrogen, Carlsbad, CA, USA) and then resuspended to an appropriate density with T lymphocyte medium, and co-cultured with target cells at various E:T ratios (10:1, 5:1, 1:1, 1:5, and 1:10) in a 96-well plate for 24 h. The 7-AAD Viability Staining Solution was used to stain dead cells and analyzed by flow cytometry. The equation used to calculate cytotoxicity percentage was 100 × (target cell death – spontaneous cell death)/(100 – spontaneous cell death).

2.9. Chronic antigen stimulation assay

T-cells were repeatedly stimulated for three consecutive weeks with γ-irradiated Nalm-6 cells at a 1:1 ratio and cultured with IL-2 supplementation. Trypan blue-stained cell counting and immunophenotypes by flow cytometry to evaluate T-cell stemness and exhaustion markers were performed weekly.

2.10. Statistical analysis

Data from a minimum of three independent experiments were collected and presented as mean ± standard deviation (SD). Statistical analysis was performed using GraphPad Prism software Version 9.5.1 (GraphPad Software, La Jolla, CA, USA). The student's *t*-test, one-way ANOVA, or two-way ANOVA with Bonferroni's or Tukey's post-test correction was used as appropriate. $P < 0.05$ was considered statistically significant.

3. Results

3.1. Generation of autologous hematopoietic stem cell-derived T lymphocytes

The peripheral blood HSCs from donor's apheresis products were cultured through a period of 52 days to generate the HSC-T (Fig. 1A). We initially isolated the $CD3^+$ and $CD34^+$ cells from PBSC samples using density gradient centrifugation and anti-CD3 or anti-CD34 magnetic beads (Fig. 1B). The percentages of pre-isolated $CD34^+$ and $CD3^+$ cells in the stem cell product were 5.9 % and 19.6 % and could reach up to 91.8 % and 86.1 % purity, respectively post-isolation (Fig. 1C and D).

We further identified the specific lineage of these HSCs according to a previous study on human hematopoietic lineage [44] using two markers, CD38 and CD133. The HSCs could then be classified into $CD38^+/CD133^+$ common lymphoid progenitor (CLP), $CD38^+/CD133^-$ erythro-myeloid progenitor (EMP), or $CD38^-/CD133^+$ lymphoid-primed multipotent progenitor (LMPP) cells (Fig. 1E). On day 0, a high proportion of $CD38^+/CD133^+$ cells up to 90.2 % of total $CD34^+$ cells were observed. After culturing for 14 days, a large fraction of $CD34^+$ and $CD38^+/CD133^+$ cells significantly decreased and most of these cells further differentiated into progenitor T-cells (Fig. 1E). Thus, these results confirmed the preservation of the CLP lineage by $CD34^+$ which could be specifically differentiated into mature T lymphocyte after culturing.

Four patients and one healthy donor were included in this study (Table S1). We first cultured the HSCs derived from the healthy donor (number 1) according to the commercially provided HSC-T generation protocol. However, the proportion of identified progenitor T-cells was 65 % on day 14, which differentiated into mature $CD3^+$ cells that represented only 8 % at the end of the culture period (Table S1). Since the original protocol aimed to differentiate double-positive cells into functionally active $CD8^+$ single-positive T-cells, interleukin-15 (IL-15) and ImmunoCult Human CD3/CD28/CD2 T Cell Activator were added into the cell culture at the final step. To the best of our knowledge, the effective CAR-T cell therapy typically uses a mixture of $CD4^+$ and $CD8^+$ T-cells to enhance CAR-T cell expansion, persistence, and potent anti-tumor activity [45–47]. Therefore, we optimized the protocol to generate both mature $CD4^+$ and $CD8^+$ T-cells from the samples of the patients (numbers 2–5). During the T-cell maturation process, we chose a protocol that activated progenitor T-cells using anti-CD3/CD28 beads instead of the human CD3/CD28/CD2 soluble bead activator on day 42 and co-cultured with T lymphocyte medium supplemented with human IL-2 instead of IL-15 for 10 days. Notably, a significant proportion of mature $CD3^+$ cells up to 82–98 % were observed in the last three patients compared to the previous protocol. Moreover, the CD8 to CD4 ratio was around 2:1, which was different from the previous studies where only $CD8^+$ cells were obtained following stem cell generation (Table S1) [29–31].

Using the optimized HSC-T generation protocol, we successfully generated HSC-T with a 3735 accumulative fold expansion from three out of the four patients (numbers 3–5) at the end of the culture period (Fig. 2A). In one patient only (number 2), who was diagnosed as diffuse large B-cell lymphoma (DLBCL) and heavily treated with multiple high-intensity chemotherapy and radiotherapy, the HSCs failed to differentiate into T lymphocytes following two trials (Table S1). The HSCs predominantly differentiated into late-stage thymocytes of progenitor T-cells ($CD5^+/CD7^+$) at percentages of 63.5 %, 74.4 %, and 90 % on days 14, 42, and 52, respectively (Fig. 2B and C). We observed the dynamic changes of dual $CD4^-/CD8^-$ or $CD4^+/CD8^+$ and transition into single $CD4^+$ or $CD8^+$ cells over time which indicated a T lymphocyte maturation process (Fig. 2C–D, S1A). Meanwhile, $CD3^+$ cells significantly matured on days 42 and 52 at 41 % and 90 %, respectively (Fig. 2B–D). At the end of the culture period, a single $CD8^+$ population was present at 53 % and a $CD4^+$ population was present at 27.3 % of the total $CD3^+$ cells (Fig. 2D). Overall, the data demonstrated the successful establishment of HSC-derived T lymphocytes using the optimized HSC generation protocol.

3.2. HSC-derived T lymphocytes revealed distinct immunophenotypes to peripheral blood-derived T lymphocytes

We assessed T-cell immunophenotypes and subsequently compared them with PB CD3-T cells to obtain additional characteristics of T-cells, differentiation subsets, and exhaustion phenotypes following the course of HSC-T generation. At the end of the culture period, the T-cell receptor (TCR) $\alpha\beta^+$, which constitutes the predominant TCR among T lymphocytes, was identified in CD3-T and HSC-T at 95.3 % and 51 %, respectively (Fig. 2E). The RA isoform of the transmembrane phosphatase CD45, lymph node homing molecule L-selectin (CD62L), and CCR7 are co-expressed on naïve T-cells (T_N) (Fig. S2A). Moreover, central memory T-cells (T_{CM}) also express CD62L and CCR7 in which effector memory T-cells (T_{EM}) lose these molecules. In this study, we simplified the assessment of the T-cell differentiation subsets using CD45RA and CD62L markers. The T-cells were systematically categorized into four distinct subsets that encompassed $CD45RA^+/CD62L^+$ T_N, $CD45RA^-/CD62L^+$ T_{CM}, $CD45RA^-/CD62L^-$ T_{EM}, and $CD45RA^+/CD62L^-$ effector memory T cells that re-expressed CD45RA (T_{EMRA}) as demonstrated in both preclinical and clinical CAR-T cell research (Fig. 3A) [45,46,48,49]. The results indicated that the CD3-T cells were equally distributed into four T-cell subsets at 34.9 %, 27.8 %, 15 %, and 28.3 % for T_N, T_{CM}, T_{EM}, and T_{EMRA}, respectively. However, the HSC-T remarkably preserved T_N immunophenotype at 73.2 % of total $CD3^+$ cells (Fig. 3B). Interestingly, all of the T_N subset demonstrated $CD62L^+/CD45RA^+/CD95^+$ T_{SCM} population in all donors (Fig. S2B). Regarding T-cell exhaustion, the HSC-T insignificantly expressed PD-1, LAG-3, and CTLA-4 exhausted molecules compared to CD3-T cells except for TIM-3 which was slightly high (Fig. 3B). To determine the effect of PD-1 expression on naïve T-cell phenotype, we further evaluated T-cell subsets in a separate $PD\text{-}1^+$ population and found that $PD\text{-}1^+$ HSC-T cells were mostly T_N cells. However, $PD\text{-}1^-$ HSC-T cells showed mixed T_N and T_{EMRA} populations (Fig. S2C).

In the realm of T-cell functionality, we conducted an ICCS assay to evaluate the ability of T-cells to secrete cytokines and cytotoxic granules. Following stimulation with anti-CD3/CD28 beads, HSC-T exhibited a predominant secretion of cytokines and cytotoxic granules compared to CD3-T cells. Specifically, the secretion levels were at 18.6 % for IFN-γ, 39.5 % for IL-2, 50.83 % for granzyme B, and 21.11 % for perforin. Remarkably, even in the absence of T-cell activators, we still observed a discernible degree of cytokine

secretion from HSC-T compared to CD3-T cells. This observation might be attributed to the recent stimulation with anti-CD3/CD28 beads during the T-cell generation protocol.

To conclude, HSC-T partly expressed TCRαβ^{+}, the naïve T-cell phenotypes were mostly preserved, and the TIM-3^{+} cells slightly increased after the HSC generation process. The distinct characteristics and immunophenotypes of HSC-T would not limit its higher ability for cytokine secretion over the CD3-T cells following TCR stimulation.

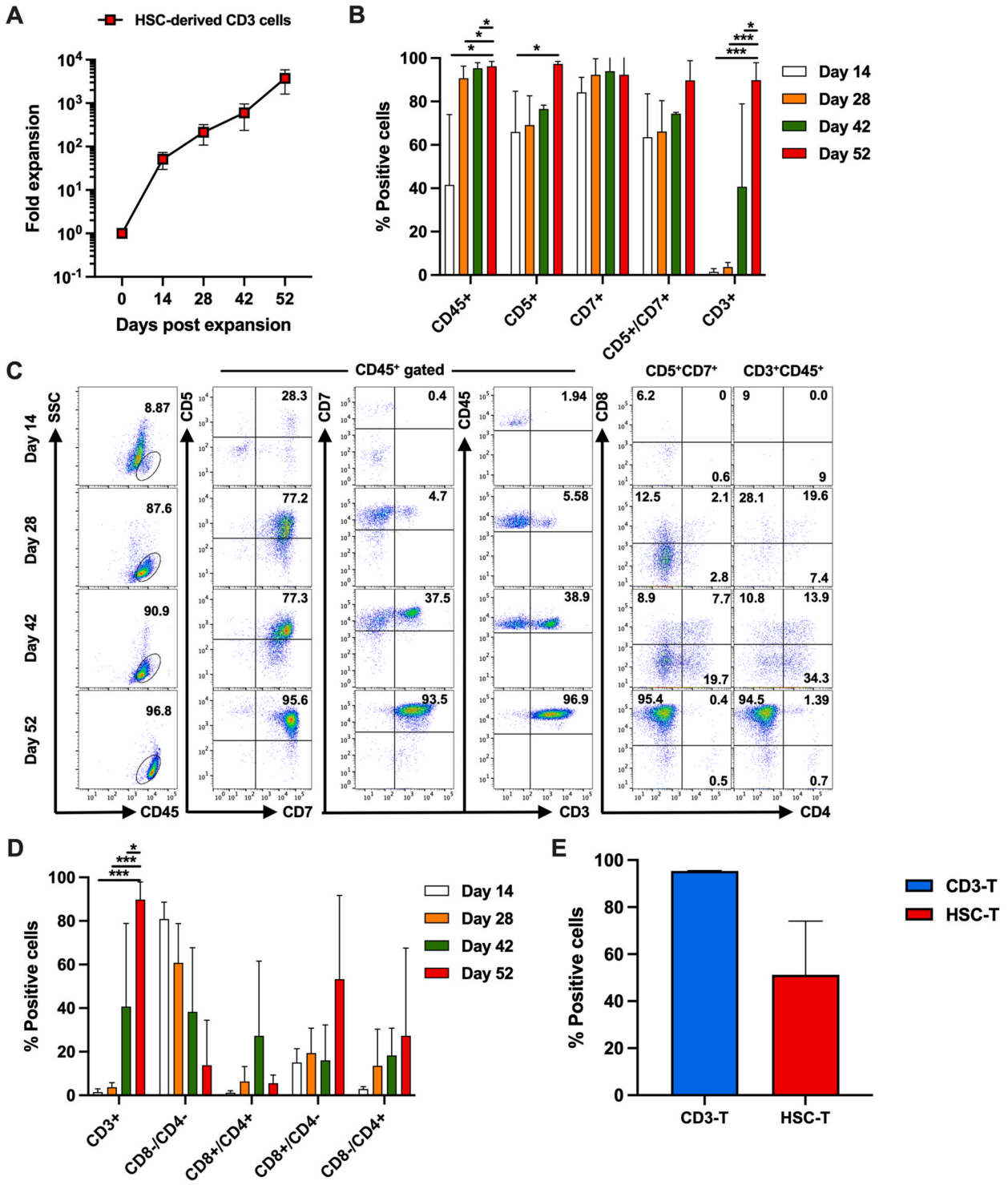

(caption on next page)

Fig. 2. HSC-derived T lymphocyte differentiation and maturation phenotypes. (A) Accumulative fold expansion of HSC-derived T lymphocyte ($CD3^+$) during the differentiation process for a total of 52 days. (B) The percentages of $CD45^+$, $CD5^+$, $CD7^+$, $CD5^+/CD7^+$, and $CD3^+$ populations during HSC-derived T lymphocyte generation at the indicated time points. (C) Representative flow plots of HSC-derived T lymphocyte at the indicated time points. Live cells were gated and the $CD45^+$ population is shown in the left column. $CD45^+$ gate (middle columns) is further classified into proportions of pan-T cells ($CD5^+$, $CD7^+$, and $CD5^+/CD7^+$) and mature T-cell ($CD3^+$) positive population. $CD5^+/CD7^+$ and $CD3^+/CD45^+$ double-positive gates are shown in the right columns to monitor subsets of single $CD8^+/CD4^-$ or $CD8^-/CD4^+$ cells, double-positive $CD8^+/CD4^+$, or double-negative $CD8^-/CD4^-$ T-cells. (D) Percentages of $CD3^+$, $CD8^-/CD4^-$, $CD8^+/CD4^+$, $CD8^+/CD4^-$, and $CD8^-/CD4^+$ populations during HSC-T lymphocyte differentiation and maturation at the indicated time points. (E) The percentages of $CD3^+/TCR\alpha\beta^+$ population of mature HSC-T or CD3-T cells. Data are pooled from three different patients and presented as mean ± SD. One-way ANOVA for (B) and (D), Student's *t*-test for (E); $^*P < 0.05$, $^{***}P < 0.001$.

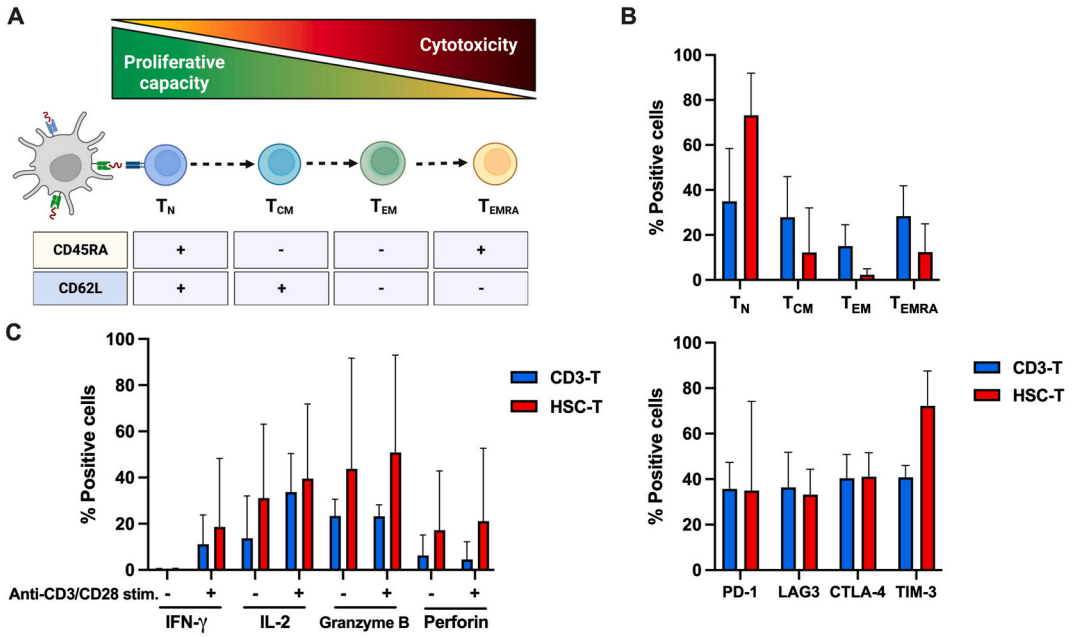

Fig. 3. T-cell immunophenotypes and functional assessment. (A) Schematic of T-cell differentiation subsets classified by a combination of CD45RA and CD62L monoclonal antibody staining to categorize T-cell subsets into naïve T (T_N) $CD45RA^+/CD62L^+$, central memory T (T_{CM}) $CD45RA^-/CD62L^+$, effector memory T (T_{EM}) $CD45RA^-/CD62L^-$, and effector memory re-expressing CD45RA T (T_{EMRA}) $CD45RA^+/CD62L^-$ cells. (B) Percentages of T-cell differentiation subset (upper panel) and T-cells expressing exhaustion phenotypes PD-1, LAG3, CTLA-4, and TIM-3 (lower panel) of mature HSC-T or CD3-T cells. (C) Intracellular cytokine staining assay for IFN-γ, IL-2, granzyme-B, and perforin of mature HSC-T and CD3-T cells at baseline or after stimulation with anti-CD3/CD28 beads at 1:1 ratio for 4 h. Data are pooled from three different patients and presented as mean ± SD. Student's *t*-test for (B), (C); P = NS.

3.3. HSC-T-derived anti-CD19 expressing CAR cells potentially demonstrated greater anti-tumoricidal activities over CD3-derived CAR-T cells

We generated genetically-modified anti-CD19 CAR-T cells using both HSC-T and CD3-T cells to assess the applicable utilization of HSC-T as a T-cell product for cancer immunotherapy. The third-generation CD19CAR with CD28/CD40 co-stimulatory domain (CD19.28.40z CAR) structure (Fig. 4A) was established by our laboratory and demonstrated superior CAR-T cell proliferation and anti-tumor activity. The results were compared to second-generation CD19CAR-T cells both *in vitro* and *in vivo* xenograft models [42]. We successfully introduced CAR gene into HSC-T and CD3-T cells with comparable transduction efficacy (range 29.11–46.50 %) and achieved greater than 90 % purity after tEGFR selection (Fig. 4B and C). The γ-irradiated EBV-LCL was used as feeder cells to expand enriched CAR-T cells, which revealed an insignificant difference in fold expansion in both types of CD19CAR-T cells (range 46.17–272.00) (Fig. 4D). Overall, both CD3-T or HSC-T were feasible T-cell sources for CD19CAR-T cell generation and could achieve high transduction efficacy and expansion following stimulation with feeder cells.

In terms of CAR-T cell function, we performed an experiment to assess the proliferative capacity of CAR-T cells by stimulating with γ-irradiated CD19-K562 and cultured in conditions of either with or without IL-2. HSC-T-derived CD19CART cells demonstrated a comparable proliferative capacity with CD3-derived CAR-T cells, whether or not supplemented with IL-2 (Fig. 5A). We then evaluated the CAR-T cell capability to release cytokines and cytotoxic granules upon exposure to target antigen by ICCS assay. Our results indicated that HSC-T-derived CAR-T cells produced significantly higher IFN-γ, in contrast, both CD3-T- and HSC-T-derived CAR-T cells exhibited a similar proportion of IL-2 positive cells. Furthermore, HSC-T-derived CD19CAR-T cells showed a tendency to have higher

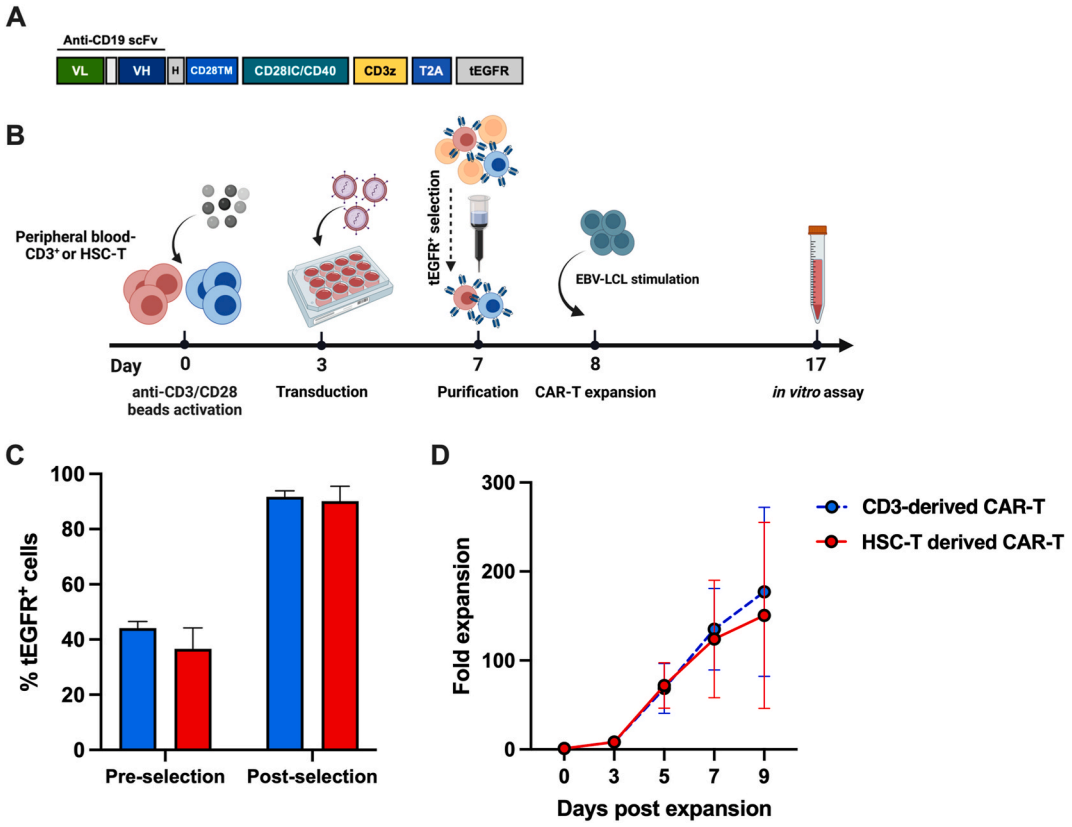

Fig. 4. CD19 chimeric antigen receptor (CAR) T-cell generation. (A) Illustration of the third-generation CD19CAR construct. Anti-CD19 scFv was fused with the hinge region (H) of the CD28 transmembrane domain (TM) followed by CD28/CD40 co-stimulatory domain and CD3ζ. A truncated version of epithelial growth factor receptor (tEGFR) was fused to the CAR structure with self-cleaving T2A sequence as a selection marker. scFv, single-chain variable fragment; VL, light chain variable fragment; VH, heavy chain variable fragment. (B) Experimental schematic of CD19CAR-T cell generation. HSC-T, hematopoietic stem cell-derived T lymphocyte; EBV-LCL, Epstein-Barr virus-transformed lymphoblastoid cell line. (C) Transduction efficacy and purification of CD19CAR-T cells pre- and post-selection. (D) CD19CAR-T cell expansion after stimulation with feeder γ-irradiated EBV-LCL at a 1:7 effector to stimulator ratio for 10 days. Data were pooled from two different patients and are shown as mean ± SD. Student's *t*-test for (C) and (D); P = NS.

percentages of granzyme B and perforin secretions compared to CD3-derived CD19CAR-T cells irrespective of antigen stimulation (Fig. 5B). We further assessed the effect of PD-1 expression on CAR-T cell functions and found that both types of CAR-T cells evenly expressed PD-1 at pre- and post-antigen stimulation (Fig. S3A). HSC-T-derived CAR-T cells again showed a tendency to have higher percentages of IFN-γ and granzyme B secretions compared to CD3-derived CAR-T cells regardless of PD-1 expression (Fig. 5C–S3B). In contrast, CD3-derived CAR-T cells demonstrated significant impairment in IFN-γ secretion following PD-1 upregulation (Fig. 5C).

Since the HSC-T cells showed only half of the TCR $\alpha\beta^+$ population after generation, we evaluated the existence of the TCR $\alpha\beta^+$ population and the responses on CAR-T cells. After CAR generation, both CD3-derived and HSC-T-derived CAR-T cells showed equivalent populations of TCR $\alpha\beta^+$ at 78.15 % and 74.3 %, respectively (Fig. S3A). Using the ICCS assay, both types of CAR-T cells produced similar levels of cytokines and cytotoxic granules among the TCR $\alpha\beta^+$ or TCR $\alpha\beta^-$ populations (Figs. S3C–D). Notably, TCR $\alpha\beta^+$ HSC-T-derived CD19CAR-T cells demonstrated greater IFN-γ secretion compared to TCR $\alpha\beta^+$ CD3-derived CAR-T cells after stimulation with CD19-positive target cells (Fig. S3C). These results emphasized the superior cytotoxic granule secretion of HSC-T-derived CD19CAR-T cells compared to CD3-derived CAR-T cell counterparts.

We conducted specific cytolysis experiments to highlight the anti-tumor function of CAR-T cells by co-culturing CD19CAR-T cells with patient-derived primary MCL cells, Nalm-6, or Raji cells. A trend of higher cytotoxicity against primary MCL cells was demonstrated by HSC-T-derived CD19CAR-T cells across all E:T ratios. However, the distinction in cytolysis against the Nalm-6 or Raji cells by CD3-derived CD19CAR-T or HSC-T-derived CD19CAR-T cells was less pronounced (Fig. 5D–S3E).

Subsequently, we performed a chronic antigen stimulation assay to evaluate the functional limit of the patient's CD3-derived CAR-T cells or HSC-T-derived CAR-T cells following repetitive exposure to CD19 antigens as *in vivo* using CAR-T cell immunophenotypes. The results showed that both types of CAR-T cells consistently displayed a high T_{EM} subset throughout the experiment with particular expression after the second stimulation (Fig. 5E). On the contrary, untransduced T-cells exhibited higher T_{EMRA} phenotype, which was indicative of a terminally differentiated T-cell subset compared to CD19CAR-T cell populations (Fig. 5E). Insignificant differences were observed in the expression of exhaustion phenotypes that included PD-1, LAG3, and CTLA-4. However, TIM-3 phenotypes tended to be

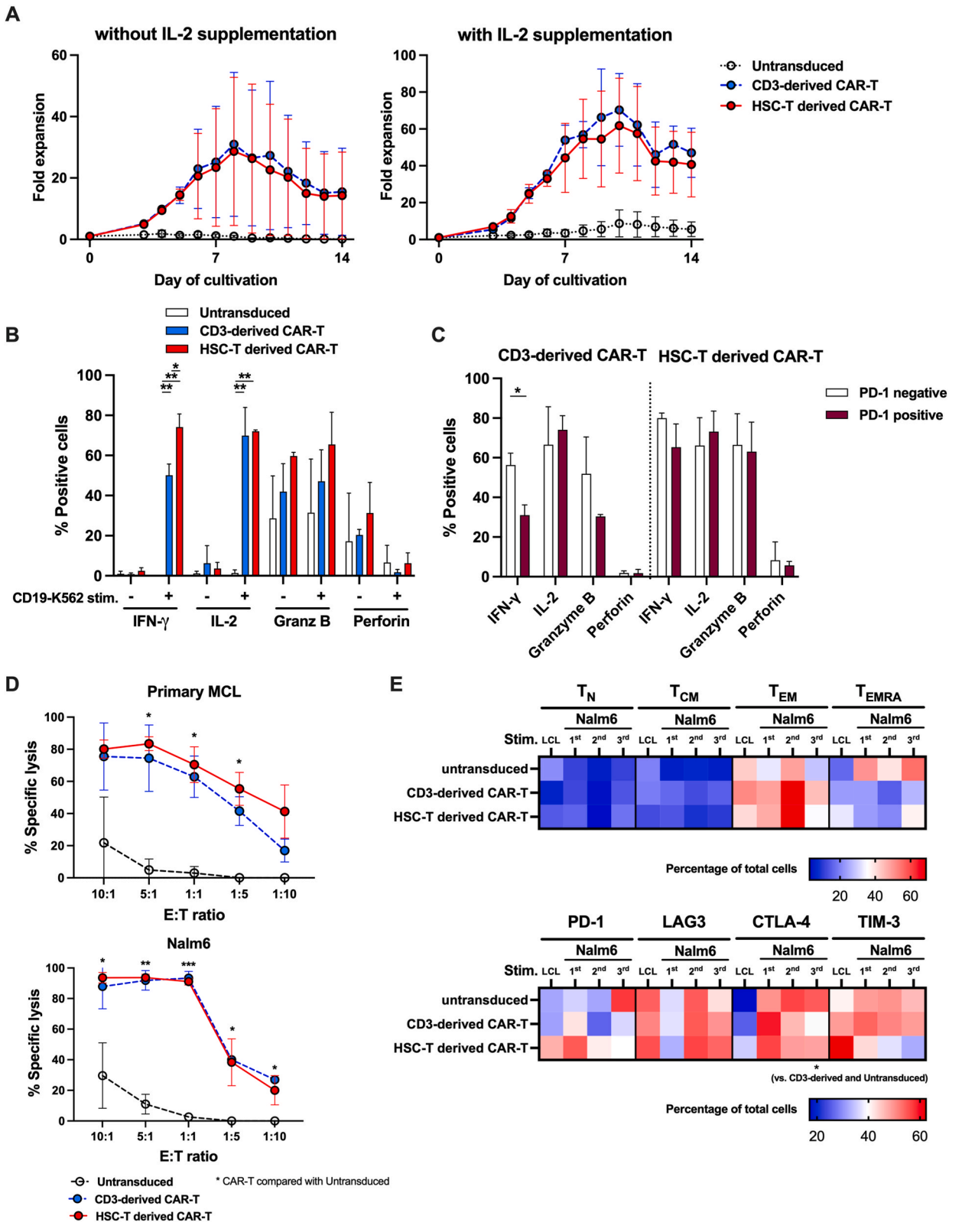

(caption on next page)

Fig. 5. Functional analysis of CD19CAR-T cell. (A) CAR-T cell proliferation assay. Untransduced-T or CD19CAR-T cells were stimulated with γ-irradiated CD19-K562 at a 1:1 ratio and cultured without (left) or with (right) IL-2 50 IU/mL for a total of 14 days. (B) Intracellular cytokine staining (ICCS) assay for IFN-γ, IL-2, granzyme-B, and perforin of untransduced-T or CD19CAR-T cells at baseline or after stimulation with CD19-K562 at a 1:2 ratio for 4 h. (C) ICCS assay for IFN-γ, IL-2, granzyme-B, and perforin of PD-1$^-$ or PD-1$^+$ CD19CAR-T cells after stimulation with CD19-K562 at a 1:2 ratio for 4 h. (D) Specific cytolysis assay. CellTrace Violet-labeled untransduced or CD19CAR-T cells were co-cultured with primary mantle cell lymphoma cells (upper panel) or Nalm-6 cells (lower panel) at various effector (E) to target (T) ratios of 10:1, 5:1, 1:1, 1:5, and 1:10 for 24 h without exogenous IL-2. The percentage of dead cells was determined by 7-AAD Viability Staining Solution and analyzed by flow cytometry. (E) Heatmap of T-cell differentiation subsets (upper panel) and T-cell expression of exhaustion phenotypes (lower panel) of untransduced-T or CD19CAR-T cells after weekly stimulation with γ-irradiated Nalm-6 cells at a 1:1 ratio (chronic antigen stimulation assay). T-cell differentiation subsets were classified by a combination of CD45RA and CD62L monoclonal antibody staining to categorize T-cell subsets into naïve T (T_N) CD45RA$^+$/CD62L$^+$, central memory T (T_{CM}) CD45RA$^-$/CD62L$^+$, effector memory T (T_{EM}) CD45RA$^-$/CD62L$^-$, and effector memory re-expressing CD45RA T (T_{EMRA}) CD45RA$^+$/CD62L$^-$ cells. T-cells expressing exhaustion phenotypes were classified as PD-1, LAG3, CTLA-4, or TIM-3 positive population. Data were pooled from two different patients and are presented as mean ± SD. One-way ANOVA for (A), (B), (D), and (E); $^*P < 0.05$, $^{**}P < 0.01$, $^{***}P < 0.001$; Student's *t*-test for (C); $^*P < 0.05$.

lower in HSC-T derived CD19CAR-T cells compared to CD3-derived CAR-T cells during the repetitive antigen stimulation period (Fig. 5E).

To conclude, HSC-T-derived CD19CAR cells were successfully generated with potentially higher anti-tumoricidal activities over CD3-derived CAR-T cells while preserving the proliferative capacity, T-cell subsets, and exhaustion phenotypes.

4. Discussion

ACT, particularly CAR-T cell, has undergone extensive investigation and now has become a principal therapeutic option for relapsed/refractory B-cell malignancies. However, various issues, which include ineffective T-cell functions and an inadequate number of collected T-cells for therapeutic purposes, are a concern in the current autologous CAR-T cell therapy model. To elucidate the unmet needs of CAR-T cell production, this study developed a strategy to generate autologous T lymphocytes from HSCs *ex vivo* and assessed the feasibility of an alternative autologous T-cell product for cellular immunotherapy.

To prove the concept, we conducted a prospective experimental study using non-cryopreserved PBSC grafts obtained from heavily pretreated patients who underwent autologous stem cell transplantation. This approach was aimed to mimic the circumstances of an individual candidate for ACT. We initially followed the available stem cell generation protocol but failed to generate mature CD3$^+$ from the HSCs derived from a healthy donor at the beginning of the pilot study. As a result, we optimized the protocol by introducing a ten-day phase of a single-positive T-cell maturation process by co-culturing progenitor T-cells with anti-CD3/CD28 and IL-2 supplementation. The remarkable results revealed mature T lymphocytes from three out of four patients with multiple myeloma or lymphoma were established. Despite the exposure to high intensity chemotherapy, the HSCs from one myeloma and two lymphoma patients were successfully differentiated into mature T lymphocytes with robust fold expansion after a long-term culture protocol mimicking T-cell differentiation in humans. However, it is important to highlight the discrepancies among the patients in terms of T-cell number, differentiation efficiency, immunophenotypes, and functions. Likewise, HSCs from one patient failed to differentiate into progenitor T-cells after 14 days of culture that normally found more than 80 % of T-cell precursors in the other patients. Additionally, the HSCs of these patients also failed to fully mature at the end of the culture period after stimulation with anti-CD3/CD28 beads in the second trial. We explored the mechanism underlying this phenomenon and discovered this patient had received multiple courses of high intensity chemoimmunotherapy and radiotherapy before transplantation which negatively suppressed the viability and stemness of the HSCs. It is well known that administration of high-dose chemotherapy causes significant injury to the bone marrow, which serves as the home of HSCs and contributes to the generation of various blood cells [50–56]. Similar to the study by Bonte and colleagues that they generated tumor antigen-specific T-cells from HSC sources; healthy donors, patients in remission after chemotherapy, and acute myeloid leukemia patients at diagnosis. Following the OP9-DL1 co-culture, they observed the significant differences in HSC-T cell numbers among donors that the patient samples could produce fewer cells compared to healthy donor samples. They concluded that the isolated human HSC from heavily-pretreated patients resulted in slower T-cell differentiation and need the multiple rounds of agonist peptide stimulation [37].

After the lymphoid progenitor differentiation phase, late-stage thymocytes of progenitor T-cells (CD5$^+$/CD7$^+$) dramatically increased and ultimately matured into CD3$^+$ cells at more than 90 % after the T-cell maturation phase. After T-cell lineage commitment in thymus, thymocytes become biased toward one of two possible lineages of TCR γδ$^+$ or TCR αβ$^+$ T-cells. In this study, the αβ$^+$ TCR was identified in half of HSC-T after the maturation process in which the negative αβ TCR population was presumed to be γδ$^+$ T-cells, the innate T lymphocytes. This could be explained by the lack of thymic cortical epithelial cells as *in vivo*, which is required for the positive selection of αβ$^+$ TCR [57–59]. The role of anti-CD3/CD28 monoclonal antibodies in γδ$^+$ T-cell expansion is still unclear. Previous studies found that CD28$^+$ γδ$^+$ T-cells had greater T-cell activation, proliferation, and cytokine secretion after stimulation with the anti-CD28 monoclonal antibody; however, some studies showed unchanged results [60–63]. Further comprehensive studies are needed to assess the CD28 co-stimulatory signals in γδ$^+$ T-cells.

Usually, T-cells predominantly express αβ$^+$ TCR, which is responsible for engaging peptide antigens presented by antigen-presenting cells in a major histocompatibility complex (MHC)-dependent manner. In contrast, γδ$^+$ TCR mainly presents on a subset of T-cells called γδ T-cells, which are located in various tissues, such as the skin, gut, and lungs. These cells can recognize different types of antigens, including peptides, lipids, and small molecules, through a mechanism independent of MHC molecules. Besides having

distinct expression and antigen recognition characteristics, $\alpha\beta^+$ TCR and $\gamma\delta^+$ TCR also have different functions in the immune system. T-cells, utilizing $\alpha\beta^+$ TCR, participate in adaptive immune responses such as activating other immune cells and generating antibodies. Meanwhile, $\gamma\delta^+$ T-cells play an innate role providing prompt response to pathogens and contribute to tissue repair and regeneration. Even though our study demonstrated only half of $\alpha\beta^+$ TCR as a proportion of all HSC-T, these T-cells preserved T-cell functions in terms of T-cell proliferation, immunophenotypes, and cytotoxicity. Moreover, the CAR-engineered T-cells are able to function independently on MHC molecules; therefore, both $\alpha\beta^+$ TCR or $\gamma\delta^+$ TCR T-cells could be adopted as T lymphocyte products as previously described [64–66]. In addition, their limited TCR repertoire and inability to recognize MHC/peptide complexes are less likely to induce GvHD in the allogeneic setting, and unlikely to cause autoimmunity. The remarkable benefit for the use of CD19CAR products as an allogeneic setting can be considered as "universal CAR-T" [64,67].

The modified HSC generation process also promoted both single $CD8^+$ and $CD4^+$ generations that gave a CD8:CD4 ratio of 2:1 at the end of the culture period. Previous studies on HSC-T manufacturing methods required multiple steps of culture and various supplemented cytokines that could achieve only a $CD8^+$ T lymphocyte product and would be unsuitable for universal ACT application [29–31]. Furthermore, HSC-T cells were mostly preserved naïve T-cell phenotype compared to CD3-T cells. The naïve T-cell subset represents a state of quiescence, long-lived or dormant T-cells which preserve T-cell proliferative capacity. This finding confirmed an absence of pre-exposure of HSC-T to antigens, unlike CD3-T cells which experience repeated exposure to antigens and potentially differentiate into memory or effector T-cell subsets [49].

We observed similar levels of PD-1 expression on CD3-T cells and HSC-T cells. A previous study demonstrated that some degree of $PD\text{-}1^+$ CD8 T-cells could be found in healthy donors that did not express transcriptional programing of T-cell exhaustion as shown in a chronic viral infection model. Moreover, these cells are not inert and have some level of residual function that are capable of producing cytokines after stimulation [68]. On the other hand, we noted a high expression of TIM-3 molecule on HSC-T cells compared to CD3-T cells. The distinct expression could be influenced by the generation process which is involved in repetitive anti-CD3/CD28 bead activation. Recent studies indicated that chronic activation of $CD8^+$ T-cells could trigger an expression of TIM-3 and served as a negative feedback mechanism to regulate and control overt T-cell activation [69–71]. However, higher innate, naïve, or $TIM\text{-}3^+$ phenotypes of HSC-T did not dampen their ability to proliferate or secrete cytokines and cytotoxic granules compared to CD3-T cells.

To ensure an applicable alternative T-cell product, we additionally generated HSC-T-derived or CD3-derived CAR cells using the CD19CAR model. The data demonstrated potentially higher cytotoxicity and cytokine secretion of HSC-T-derived CD19CAR cells over CD3-derived CD19CAR-T cells following stimulation with $CD19^+$ target cells as shown in superior specific cytolysis against primary MCL. We noticed that the proportion of IFN-γ-secreted $PD\text{-}1^+$ CD3-derived CAR-T cells diminished upon stimulation with $CD19^+$ antigen. This was illustrated by a negative correlation between the exhausted T-cells and IFN-γ secretion which represents ineffective T-cell function of heavily pretreated patients. Moreover, HSC-T-derived CD19CAR cells sustained their T-cell proliferation, stemness, or exhaustion phenotypes in the repetitive antigen stimulation assay comparable to control CD19CAR-T cells. In particular, different fold expansions among the patients of HSC-T- or CD3-derived CAR-T cells in the proliferation assay were observed. This might again be explained by the distinct history of chemotherapeutic exposure that was shown to influence ineffective T-cell proliferative capacity [72].

Extensive studies on the generation of T lymphocytes from UCB, HSCs, or iPSCs using stromal co-culture or feeder-free system have been proposed [29,37–39,41,73–75]. This current study demonstrated the generation of T lymphocytes from patient autologous HSCs using stromal-free culture system. Furthermore, this feasible generation process showed comparable T-cell functions to patient CD3 cells. We also revealed the applicable utilization of HSC-T as an alternative T-cell product for adoptive CAR-T cell therapy. Previous studies focused on procedures that used USB or HSC derived-T-cells from healthy donors. The processes were complicated and laborious and required multiple stages that used diverse cytokines, which would make them difficult to implement in real-world settings. Additionally, the final cell products were CD8 T-cells or NK cells which have superior cytotoxicity but limited persistence, especially NK cells [29–31].

The clonality of HSC-derived T-cells is also crucial concern. We did not assess the TCR repertoire of CD3-T or HSC-T cells in the current study; however, there are evidences of iPSC- or HSC-derived T-cells express characteristics of TCR polyclonality. The study by Chang and colleagues generated T-cells from iPSC with confirmed a diverse range of TCR Vβ segments and diverse CDR3 sequences, indicating a broad TCR repertoire [76]. A recent study by Singh et al. demonstrated the *in vitro* StemRegenin-1 expanded progenitor T-cells from $CD34^+$ human HSCs retained T-cell functions with polyclonal TCR repertoire similar to $CD3^+$ naïve T-cells isolated from periphery of engrafted mice [75]. Moirangthem and colleagues also confirmed that the mature $CD3^+$ cells (expressing γδ or αβ TCRs) generated from TNFα-treated cord blood or mobilized peripheral blood human T-lymphoid progenitor cells which were co-cultured with OP9-DL1 cells gave rise the polyclonal TCR repertoire without any bias [41].

This study has a few limitations. First, we generated HSC-T from a small number of samples. Also, the subtypes of the hematologic diseases were nearly uniform, i.e., myeloma or lymphoma, which would affect the study results and, therefore, could not universally represent HSC-T characteristics. Moreover, the cytolysis against resistant cellular models and *in vivo* HSC-derived CAR-T cell functions and TCR clonality of HSC-derived T-cells were beyond the scope of this current research. Due to the limited resources, we did not assess the proportion of TCR $\gamma\delta^+$ population after HSC-T cell generation. A large-scale generation of HSC-T, larger numbers of patients and diseases, as well as *in vivo* HSC-derived CAR-T cell functions are needed to confirm the results of this study for application in real-world clinical settings. Long-term culture conditions to generate HSC-T are obviously not cost-effective in clinics; however, this strategy would offer a great opportunity for patients with an inadequate number of T-cells to access ACT. In the next step, efforts will focus on improvements and shortening the duration of HSC-T generation as well as scaling up the manufacturing process to extend product efficiency.

5. Conclusions

In summary, we successfully generated HSC-derived T lymphocytes from patient autologous HSCs with preserved T-cell efficacy. The HSC-T cells are potentially utilized as an alternative option for cellular immunotherapy.

Financial support

The research was granted by the Faculty of Medicine (Grant No.65-001-3; REC 65-315-14-1 to J.J.), Prince of Songkla University, and National Research Council of Thailand (NRCT) (Grant No. N35E660102 to J.J.). K.M. was supported by Graduate Scholarship (Grant No. 64-003-1). J.J. was supported by Royal King Ananda Mahidol Foundation Scholarship for Research Scholar.

Ethics approval and consent to participate

The research protocol was approved by the Human Research Ethics Committee of the Faculty of Medicine, Prince of Songkla University, Thailand (REC.65-315-14-1). Apheresis HSC products were obtained from a healthy donor or multiple myeloma or lymphoma patients who underwent stem cell transplantation. Primary mantle cell lymphoma (MCL) cells were obtained from a patient with MCL.

Consent for publication

All authors have read the manuscript and provided their consent for the submission.

Data availability statement

All data generated or analyzed during this study are included in this published article (and its Supplementary files) and available from the corresponding author on reasonable request.

CRediT authorship contribution statement

Kajornkiat Maneechai: Writing – review & editing, Writing – original draft, Validation, Methodology, Investigation, Formal analysis, Data curation, Conceptualization. **Wannakorn Khopanlert:** Writing – review & editing, Resources, Methodology, Investigation. **Panarat Noiperm:** Writing – review & editing, Resources, Investigation. **Phakaporn Udomsak:** Writing – review & editing, Resources, Investigation. **Pongtep Viboonjuntra:** Writing – review & editing, Resources, Investigation. **Jakrawadee Julamanee:** Writing – review & editing, Writing – original draft, Visualization, Validation, Supervision, Software, Resources, Project administration, Methodology, Investigation, Funding acquisition, Formal analysis, Data curation, Conceptualization.

Declaration of competing interest

The authors declare that they have no known competing financial interests or personal relationships that could have appeared to influence the work reported in this paper.

Acknowledgements

The authors thank Stem Cell Laboratory, Department of Biomedical Science and Bioengineering, and Translational Medicine Research Center, Faculty of Medicine, Prince of Songkla University for technical assistance. The research was granted by the Faculty of Medicine (Grant No.65-001-3; REC 65-315-14-1 to J.J.), Prince of Songkla University, and National Research Council of Thailand (NRCT) (Grant No. N35E660102 to J.J.). K.M. was supported by Graduate Scholarship (Grant No. 64-003-1). J.J. was supported by Royal King Ananda Mahidol Foundation Scholarship for Research Scholar. The abstract of this manuscript was presented at the 49th European Blood and Marrow Transplantation Annual Meeting, Paris, France.

Appendix A. Supplementary data

Supplementary data to this article can be found online at https://doi.org/10.1016/j.heliyon.2024.e38447.

References

[1] A.I. Salter, M.J. Pont, S.R. Riddell, Chimeric antigen receptor-modified T cells: CD19 and the road beyond, Blood 131 (24) (2018) 2621–2629.
[2] M.L. Davila, et al., Efficacy and toxicity management of 19-28z CAR T cell therapy in B cell acute lymphoblastic leukemia, Sci. Transl. Med. 6 (224) (2014) 224ra25.

[3] S.L. Maude, et al., Chimeric antigen receptor T cells for sustained remissions in leukemia, N. Engl. J. Med. 371 (16) (2014) 1507–1517.
[4] D.W. Lee, et al., T cells expressing CD19 chimeric antigen receptors for acute lymphoblastic leukaemia in children and young adults: a phase 1 dose-escalation trial, Lancet 385 (9967) (2015) 517–528.
[5] J.S. Abramson, et al., Lisocabtagene maraleucel for patients with relapsed or refractory large B-cell lymphomas (TRANSCEND NHL 001): a multicentre seamless design study, Lancet 396 (10254) (2020) 839–852.
[6] D.L. Porter, et al., Chimeric antigen receptor T cells persist and induce sustained remissions in relapsed refractory chronic lymphocytic leukemia, Sci. Transl. Med. 7 (303) (2015) 303ra139.
[7] J.N. Kochenderfer, et al., Chemotherapy-refractory diffuse large B-cell lymphoma and indolent B-cell malignancies can be effectively treated with autologous T cells expressing an anti-CD19 chimeric antigen receptor, J. Clin. Oncol. 33 (6) (2015) 540–549.
[8] S.J. Schuster, et al., Chimeric antigen receptor T cells in refractory B-cell lymphomas, N. Engl. J. Med. 377 (26) (2017) 2545–2554.
[9] S.S. Neelapu, et al., Axicabtagene ciloleucel CAR T-cell therapy in refractory large B-cell lymphoma, N. Engl. J. Med. 377 (26) (2017) 2531–2544.
[10] C.J. Turtle, et al., Durable molecular remissions in chronic lymphocytic leukemia treated with CD19-specific chimeric antigen receptor-modified T cells after failure of ibrutinib, J. Clin. Oncol. 35 (26) (2017) 3010–3020.
[11] F.L. Locke, et al., Axicabtagene ciloleucel as second-line therapy for large B-cell lymphoma, N. Engl. J. Med. 386 (7) (2022) 640–654.
[12] J.S. Abramson, et al., Lisocabtagene maraleucel as second-line therapy for large B-cell lymphoma: primary analysis of the phase 3 TRANSFORM study, Blood 141 (14) (2023) 1675–1684.
[13] S.L. Maude, et al., Tisagenlecleucel in children and young adults with B-cell lymphoblastic leukemia, N. Engl. J. Med. 378 (5) (2018) 439–448.
[14] A. Mullard, FDA approves first CAR T therapy, Nat. Rev. Drug Discov. 16 (10) (2017) 669.
[15] W. Qasim, Genome-edited allogeneic donor "universal" chimeric antigen receptor T cells, Blood 141 (8) (2023) 835–845.
[16] W. Qasim, et al., Molecular remission of infant B-ALL after infusion of universal TALEN gene-edited CAR T cells, Sci. Transl. Med. 9 (374) (2017).
[17] E. Liu, et al., Use of CAR-transduced natural killer cells in CD19-positive lymphoid tumors, N. Engl. J. Med. 382 (6) (2020) 545–553.
[18] M.M. Berrien-Elliott, M.T. Jacobs, T.A. Fehniger, Allogeneic natural killer cell therapy, Blood 141 (8) (2023) 856–868.
[19] A. Makkouk, et al., Off-the-shelf Vδ1 gamma delta T cells engineered with glypican-3 (GPC-3)-specific chimeric antigen receptor (CAR) and soluble IL-15 display robust antitumor efficacy against hepatocellular carcinoma, J Immunother Cancer 9 (12) (2021).
[20] A. Capsomidis, et al., Chimeric antigen receptor-engineered human gamma delta T cells: enhanced cytotoxicity with retention of cross presentation, Mol. Ther. 26 (2) (2018) 354–365.
[21] F. Cichocki, S.J.C. van der Stegen, J.S. Miller, Engineered and banked iPSCs for advanced NK- and T-cell immunotherapies, Blood 141 (8) (2023) 846–855.
[22] G. Awong, et al., Characterization in vitro and engraftment potential in vivo of human progenitor T cells generated from hematopoietic stem cells, Blood 114 (5) (2009) 972–982.
[23] M. Kennedy, et al., T lymphocyte potential marks the emergence of definitive hematopoietic progenitors in human pluripotent stem cell differentiation cultures, Cell Rep. 2 (6) (2012) 1722–1735.
[24] D.D. Dervovic, et al., Comparative and functional evaluation of in vitro generated to ex vivo CD8 T cells, J. Immunol. 189 (7) (2012) 3411–3420.
[25] R.N. La Motte-Mohs, E. Herer, J.C. Zúñiga-Pflücker, Induction of T-cell development from human cord blood hematopoietic stem cells by Delta-like 1 in vitro, Blood 105 (4) (2005) 1431–1439.
[26] S. Van Coppernolle, et al., Functionally mature CD4 and CD8 TCRalphabeta cells are generated in OP9-DL1 cultures from human CD34+ hematopoietic cells, J. Immunol. 183 (8) (2009) 4859–4870.
[27] B. Grzywacz, et al., Coordinated acquisition of inhibitory and activating receptors and functional properties by developing human natural killer cells, Blood 108 (12) (2006) 3824–3833.
[28] R. Haddad, et al., Molecular characterization of early human T/NK and B-lymphoid progenitor cells in umbilical cord blood, Blood 104 (13) (2004) 3918–3926.
[29] N. Boyd, et al., 'Off-the-Shelf' immunotherapy: manufacture of CD8, Cells 10 (10) (2021).
[30] S.N. De Oliveira, et al., Modification of hematopoietic stem/progenitor cells with CD19-specific chimeric antigen receptors as a novel approach for cancer immunotherapy, Hum. Gene Ther. 24 (10) (2013) 824–839.
[31] G. Awong, et al., Human CD8 T cells generated in vitro from hematopoietic stem cells are functionally mature, BMC Immunol. 12 (2011) 22.
[32] A. Zhen, et al., HIV-Specific immunity derived from chimeric antigen receptor-engineered stem cells, Mol. Ther. 23 (8) (2015) 1358–1367.
[33] F. Giannoni, et al., Allelic exclusion and peripheral reconstitution by TCR transgenic T cells arising from transduced human hematopoietic stem/progenitor cells, Mol. Ther. 21 (5) (2013) 1044–1054.
[34] I.M. Barber-Axthelm, et al., Stem cell-derived CAR T cells traffic to HIV reservoirs in macaques, JCI Insight 6 (1) (2021).
[35] A.C. Trotman-Grant, et al., DL4-μbeads induce T cell lineage differentiation from stem cells in a stromal cell-free system, Nat. Commun. 12 (1) (2021) 5023.
[36] S. Strubbe, T. Taghon, Modeling of human T cell development in vitro as a read-out for hematopoietic stem cell multipotency, Biochem. Soc. Trans. 49 (5) (2021) 2113–2122.
[37] S. Bonte, et al., T-cells with a single tumor antigen-specific T-cell receptor can be generated, OncoImmunology 9 (1) (2020) 1727078.
[38] S. Bonte, et al., OP9-DL1 co-culture and subsequent maturation in the presence of IL-21 generates tumor antigen-specific T cells with a favorable less-differentiated phenotype and enhanced functionality, OncoImmunology 10 (1) (2021) 1954800.
[39] S. Snauwaert, et al., In vitro generation of mature, naive antigen-specific CD8(+) T cells with a single T-cell receptor by agonist selection, Leukemia 28 (4) (2014) 830–841.
[40] C. Reimann, et al., Human T-lymphoid progenitors generated in a feeder-cell-free Delta-like-4 culture system promote T-cell reconstitution in NOD/SCID/γc(-/-) mice, Stem Cell. 30 (8) (2012) 1771–1780.
[41] R.D. Moirangthem, et al., A DL-4- and TNFα-based culture system to generate high numbers of nonmodified or genetically modified immunotherapeutic human T-lymphoid progenitors, Cell. Mol. Immunol. 18 (7) (2021) 1662–1676.
[42] W. Khopanlert, et al., Co-stimulation of CD28/CD40 signaling molecule potentiates CAR-T cell efficacy and stemness, Mol Ther Oncol 32 (3) (2024) 200837.
[43] J. Julamanee, et al., Composite CD79A/CD40 co-stimulatory endodomain enhances CD19CAR-T cell proliferation and survival, Mol. Ther. 29 (9) (2021) 2677–2690.
[44] A. Görgens, et al., New relationships of human hematopoietic lineages facilitate detection of multipotent hematopoietic stem and progenitor cells, Cell Cycle 12 (22) (2013) 3478–3482.
[45] D. Sommermeyer, et al., Chimeric antigen receptor-modified T cells derived from defined CD8+ and CD4+ subsets confer superior antitumor reactivity in vivo, Leukemia 30 (2) (2016) 492–500.
[46] C.J. Turtle, et al., CD19 CAR-T cells of defined CD4+:CD8+ composition in adult B cell ALL patients, J. Clin. Invest. 126 (6) (2016) 2123–2138.
[47] J.J. Melenhorst, et al., Decade-long leukaemia remissions with persistence of CD4, Nature 602 (7897) (2022) 503–509.
[48] J. Eyquem, et al., Targeting a CAR to the TRAC locus with CRISPR/Cas9 enhances tumour rejection, Nature 543 (7643) (2017) 113–117.
[49] L. Gattinoni, C.A. Klebanoff, N.P. Restifo, Paths to stemness: building the ultimate antitumour T cell, Nat. Rev. Cancer 12 (10) (2012) 671–684.
[50] D. Dumenil, et al., Some effects of chemotherapeutic drugs. III. Short- and long-term effects of cis-platinum on various hematopoietic compartments and on the kidney of the mouse, Cancer Chemother. Pharmacol. 8 (3) (1982) 267–270.
[51] D. Duménil, F. Sainteny, E. Frindel, Some effects of chemotherapeutic drugs on bone marrow stem cells. II. Effect on non-Hodgkin lymphoma chemotherapy on various hemopoietic compartments of the mouse, Cancer Chemother. Pharmacol. 2 (3) (1979) 203–207.
[52] C.E. Fadul, et al., Immune modulation effects of concomitant temozolomide and radiation therapy on peripheral blood mononuclear cells in patients with glioblastoma multiforme, Neuro Oncol. 13 (4) (2011) 393–400.
[53] R. Verma, et al., Lymphocyte depletion and repopulation after chemotherapy for primary breast cancer, Breast Cancer Res. 18 (1) (2016) 10.
[54] F.F. Fagnoni, et al., T-cell dynamics after high-dose chemotherapy in adults: elucidation of the elusive CD8+ subset reveals multiple homeostatic T-cell compartments with distinct implications for immune competence, Immunology 106 (1) (2002) 27–37.

[55] F.T. Hakim, et al., Constraints on CD4 recovery postchemotherapy in adults: thymic insufficiency and apoptotic decline of expanded peripheral CD4 cells, Blood 90 (9) (1997) 3789–3798.
[56] N.T.H. Truong, et al., Effects of chemotherapy agents on circulating leukocyte populations: potential implications for the success of CAR-T cell therapies, Cancers 13 (9) (2021).
[57] J.H. Park, H.K. Lee, Function of γδ T cells in tumor immunology and their application to cancer therapy, Exp. Mol. Med. 53 (3) (2021) 318–327.
[58] S. Paul, Shilpi, G. Lal, Role of gamma-delta (γδ) T cells in autoimmunity, J. Leukoc. Biol. 97 (2) (2015) 259–271.
[59] L.S. Lamb, R.D. Lopez, Gammadelta T cells: a new frontier for immunotherapy? Biol. Blood Marrow Transplant. 11 (3) (2005) 161–168.
[60] J.C. Ribot, et al., B7-CD28 costimulatory signals control the survival and proliferation of murine and human γδ T cells via IL-2 production, J. Immunol. 189 (3) (2012) 1202–1208.
[61] A.I. Sperling, et al., CD28-mediated costimulation is necessary for the activation of T cell receptor-gamma delta+ T lymphocytes, J. Immunol. 151 (11) (1993) 6043–6050.
[62] S.M. Hayes, P.E. Love, Distinct structure and signaling potential of the gamma delta TCR complex, Immunity 16 (6) (2002) 827–838.
[63] V. Lafont, et al., Tumor necrosis factor-alpha production is differently regulated in gamma delta and alpha beta human T lymphocytes, J. Biol. Chem. 275 (25) (2000) 19282–19287.
[64] M. Rozenbaum, et al., Gamma-Delta CAR-T cells show CAR-directed and independent activity against leukemia, Front. Immunol. 11 (2020) 1347.
[65] R.H. Vonderheide, C.H. June, Engineering T cells for cancer: our synthetic future, Immunol. Rev. 257 (1) (2014) 7–13.
[66] Z. Sebestyen, et al., Translating gammadelta (γδ) T cells and their receptors into cancer cell therapies, Nat. Rev. Drug Discov. 19 (3) (2020) 169–184.
[67] P. Vantourout, A. Hayday, Six-of-the-best: unique contributions of γδ T cells to immunology, Nat. Rev. Immunol. 13 (2) (2013) 88–100.
[68] J. Duraiswamy, et al., Phenotype, function, and gene expression profiles of programmed death-1(hi) CD8 T cells in healthy human adults, J. Immunol. 186 (7) (2011) 4200–4212.
[69] E.J. Wherry, T cell exhaustion, Nat. Immunol. 12 (6) (2011) 492–499.
[70] J. Fourcade, et al., Upregulation of Tim-3 and PD-1 expression is associated with tumor antigen-specific CD8+ T cell dysfunction in melanoma patients, J. Exp. Med. 207 (10) (2010) 2175–2186.
[71] S.F. Ngiow, et al., Anti-TIM3 antibody promotes T cell IFN-γ-mediated antitumor immunity and suppresses established tumors, Cancer Res. 71 (10) (2011) 3540–3551.
[72] K. Beider, et al., Molecular and functional signatures associated with CAR T cell exhaustion and impaired clinical response in patients with B cell malignancies, Cells 11 (7) (2022).
[73] C.S. Seet, et al., Generation of mature T cells from human hematopoietic stem and progenitor cells in artificial thymic organoids, Nat. Methods 14 (5) (2017) 521–530.
[74] M.J. Smith, et al., In vitro T-cell generation from adult, embryonic, and induced pluripotent stem cells: many roads to one destination, Stem Cell. 33 (11) (2015) 3174–3180.
[75] J. Singh, et al., Generation and function of progenitor T cells from StemRegenin-1-expanded CD34+ human hematopoietic progenitor cells, Blood Adv 3 (20) (2019) 2934–2948.
[76] C.W. Chang, et al., Broad T-cell receptor repertoire in T-lymphocytes derived from human induced pluripotent stem cells, PLoS One 9 (5) (2014) e97335.